

Algorithms for Detecting Nearby Loss of Generation Events for Decentralized Controls

Niraj Dahal, *Student Member, IEEE*, and Steven M. Rovnyak, *Member, IEEE*

Abstract—The paper describes algorithms to screen real-time frequency data for detecting nearby loss of generation events. Results from Fourier calculation are combined with other features to effectively distinguish a nearby loss of generation from similar remote disturbances. Nearby in this context usually refers to an event occurring around 50-100 miles from the measurement location. The proposed algorithm can be trained using pattern recognition tools like decision trees to enable smart devices including appliances like residential air conditioners and dryers to autonomously detect and estimate the source of large frequency disturbances. An area of application of this strategy is to actuate controls such as location targeted under frequency load shedding (UFLS) so that loads closest to a tripped generator are the most likely to shut down.

I. INTRODUCTION

A power system is a highly non-linear system. A small disturbance such as step change in load at any operating condition mostly make the system oscillate around the equilibrium. In the presence of enough damping, the system eventually remains stable. However, large transmission level disturbances like short circuit faults, line trips and re-closure, loss of large load or generation, etc. excite prolonged oscillations making one or more generators prone to losing stability. The oscillations are typically anywhere in the order of 0.1 Hz to 2 Hz. A widely researched range for local modes is 0.7-2.0 Hz while the whole interconnection mode ranges from 0.1-0.6 Hz [1], [2].

In case of large disturbances like loss of generation, there is an average decrease in electro-mechanical frequency. This paper combines the average frequency drop with the results from a Fourier calculation to detect a loss of generation event. Pattern recognition tools like decision trees (DTs) can be trained to distinguish nearby loss of generation events. Nearby events here refer to events occurring around 50-100 miles from the measurement location. An area of application of this strategy is to actuate controls such as location-targeted under-frequency load shedding (UFLS) using only local frequency measurements. The UFLS strategy of disconnecting loads near loss of generation events is intended to help prevent transmission line relays from tripping on overload by reducing phase angle differences [3]. Many blackouts result from cascading outages that involve generators and transmission lines tripping off-line due to protective relaying. This proposed strategy is

This material is based upon the work supported by the National Science Foundation under Award ECCS-1711521.

N. Dahal and S.M. Rovnyak are with the Department of Electrical and Computer Engineering, Indiana University-Purdue University Indianapolis, Indianapolis, IN 46202 USA (e-mail: srovnyak@iupui.edu)

targeted towards making these failure modes less likely to occur.

A widely used relay for UFLS is based on the rate of change of frequency (df/dt) [4], [5]. But there are limitations to the df/dt algorithm. First, the df/dt relay alone does not distinguish between shared or location-targeted load-shedding. Secondly, since df/dt is affected by the system's inertial constant (H), a high penetration of renewable energy such as wind-energy farm will significantly affect the df/dt relay's threshold [4]. Also, methods based on df/dt are susceptible to distortion by local dynamics such as glitches. The algorithms used in this paper are based on detecting the presence of local modes and are better for distinguishing a small close event from a large event. The proposed methods can accurately detect transmission level disturbances that excite local modes on the order of about 1 Hz without triggering falsely from glitches.

The results in this paper are obtained from recorded voltage measurements sampled at 720 Hz from the authors' own residence wall-outlet. An industry grade data acquisition (DAQ) card is used for continuous voltage measurement. Unlike wide-area frequency monitoring network (FNET) [6], the measurements here are captured from a single channel and no GPS synchronization or central communication is required. The authors are currently using event reports from FNET/GridEye to train and validate the proposed UFLS scheme. In actual operation, however, the trained UFLS scheme will only use local measurements without relying on GPS synchronization or central communication.

The following section discusses several indices that can be used for pattern recognition to detect nearby loss of generation events.

II. INDICES FOR DETECTING NEARBY LOSS OF GENERATION

A. Average Change in Frequency Index ($J_{\Delta f}$)

The index based on Δf is equivalent to the Haar wavelet coefficients discussed in [7], [8]. The equivalent wavelet can be formulated as—

$$\Psi(t_N) = \begin{cases} -1/N & 0 \leq t_N \leq N_s \\ +1/N & N_s < t_N \leq N \\ 0 & \text{otherwise} \end{cases} \quad (1)$$

where the number of samples (N) is assumed even and equal to $2N_s$.

The acceptability i.e. $\sum_{i=0}^N \Psi(t_i) = 0$ is necessary to rightly detect average change in frequency from their nominal value.

The performance index can be found using an inner product with frequency measurements-

$$J_{\Delta f}(t_N) = \langle f(t_N), \Psi(t_N) \rangle$$

Using (1), the inner product can be expanded as-

$$J_{\Delta f}(t_N) = \sum_{n=N+1-N_s}^N f(t_n)/N - \sum_{n=N+1-2N_s}^{N-N_s} f(t_n)/N \quad (2)$$

B. Discrete Fourier Transform Index (J_{DFT})

A local generator trip causes intra-area swings among nearby generators causing a prominent 0.8 Hz oscillations. This property is combined with results from $J_{\Delta f}$ index to detect a nearby loss of generation. The presence of 0.8 Hz oscillations can be found by inspecting the correlation of the input sequence with sine and cosine coefficients. This is similar to the 1 Hz oscillation analysis for detecting unintentional islanding in [9]. Assuming 60 samples per second, the period is 75 samples which can be rounded to $N_s = 74$ for convenience. If we define vectors V_c , V_s , V_{60} and the most recent input vector $V(t_N)$ as follows:

$$V_c = \begin{bmatrix} \cos(1\pi/37) \\ \cos(2\pi/37) \\ \dots \\ \cos(74\pi/37) \end{bmatrix}, V_s = \begin{bmatrix} \sin(1\pi/37) \\ \sin(2\pi/37) \\ \dots \\ \sin(74\pi/37) \end{bmatrix}$$

$$V_{60} = \begin{bmatrix} 60 \\ 60 \\ \dots \\ 60 \end{bmatrix}, V(t_N) = \begin{bmatrix} v(t_N - 74/60) \\ v(t_N - 73/60) \\ \dots \\ v(t_N - 1/60) \end{bmatrix}$$

the 0.8 Hz sine and cosine components Y_s and Y_c of the normalized signal can be calculated using the inner product as:

$$Y_s(t_N) = (2/74) \langle V(t_N) - V_{60}, V_s \rangle$$

$$Y_c(t_N) = (2/74) \langle V(t_N) - V_{60}, V_c \rangle$$

The magnitude of the 0.8 Hz index is then

$$J_{DFT}(t_N) = \sqrt{Y_s^2(t_N) + Y_c^2(t_N)}$$

C. Sinc Function Index (J_{sinc})

Owing to the assumption that a nearby loss of generation possibly has a set of local modes instead of just the 0.8 Hz oscillations, we use a perfect *sinc* bandpass filter that retains frequency within the band $4 < |w| < 6$ rad/sec. The continuous-time function for the band pass filtering is defined as-

$$f(t) = 6 \frac{\sin(6t)}{(6\pi t)} - 4 \frac{\sin(4t)}{(4\pi t)} \quad (3)$$

If we define vectors V_{sinc} , V_{60} and $V(t_N)$ for a 16 seconds window as follows:

$$V_{sinc} = \begin{bmatrix} f(1/60) \\ f(2/60) \\ \dots \\ f(1000/60) \\ f(1001/60) \end{bmatrix}$$

$$V_{60} = \begin{bmatrix} 60 \\ 60 \\ \dots \\ 60 \end{bmatrix}, V(t_N) = \begin{bmatrix} v(t_N - 1001/60) \\ v(t_N - 1000/60) \\ \dots \\ v(t_N - 1/60) \end{bmatrix}$$

the output of the bandpass filter V_{BP} can be calculated using the inner product of *sinc* coefficients with normalized input-

$$V_{BP}(t_N) = \langle V(t_N) - V_{60}, V_{sinc} \rangle$$

The *sinc* index (J_{sinc}) is then obtained as root mean square average of V_{BP} over 2.5 seconds.

$$J_{sinc}(t_N) = \sqrt{\frac{\sum_{k=N-149}^N V_{BP}(t_k)^2}{150}} \quad (4)$$

D. The Composite Index (J_{comp})

Our preliminary investigations used a composite index (J_{comp}), which is a linear combination of $J_{\Delta f}$ and J_{DFT} , to search recorded data for nearby loss of generation events.

$$J_{comp} = \alpha J_{DFT} - \beta J_{\Delta f} \quad (5)$$

Through experimentation, we found that a combination of parameters such as $\alpha = 0.5$ and $\beta = 1$ worked reasonably well for identifying events with the characteristic features of nearby loss of generation events. A large value of the $J_{\Delta f}$ index indicates a loss of generation and a large value of the J_{DFT} index indicates 0.8 Hz oscillation. Since we were interested in finding loss of generation events with and without oscillations, we adjusted the coefficients so that the maximum values of $\beta J_{\Delta f}$ were somewhat larger than the maximum values of αJ_{DFT} . Section III-C illustrates some issues involved in choosing parameter values for the composite index. While the composite index was useful for searching large amounts of recorded data before we had access to event reports from FNET/GridEye, the linear combination coefficients will be less important going forward because DTs will eventually be trained to apply separate thresholds to the $J_{\Delta f}$ and J_{DFT} indices.

III. CASE STUDY

A. Loss of generation: nearby versus remote events

Previous work has shown that changes in steady-state frequency can be used to detect events involving loss of generation [10]. As the authors of [10] pointed out, an index such as $J_{\Delta f}$ does not indicate the disconnection of a transmission line the way it indicates a loss of generation. The objective of the present work is to distinguish between *nearby* and *remote* loss of generation events by detecting the presence of local oscillation modes during a loss of generation event. The eventual aim of the present work is to use the detection of nearby loss of generation events for location-targeted UFLS.

A loss of 500 MW is simulated in a simplified 29-machine model of WECC and rotor frequencies are observed for nearby and remote generator buses. The nearby buses are selected from the same cluster where the generation loss has occurred while the remote buses are chosen from other clusters [11]. Fig. 1 shows presence of strong local modes of oscillations

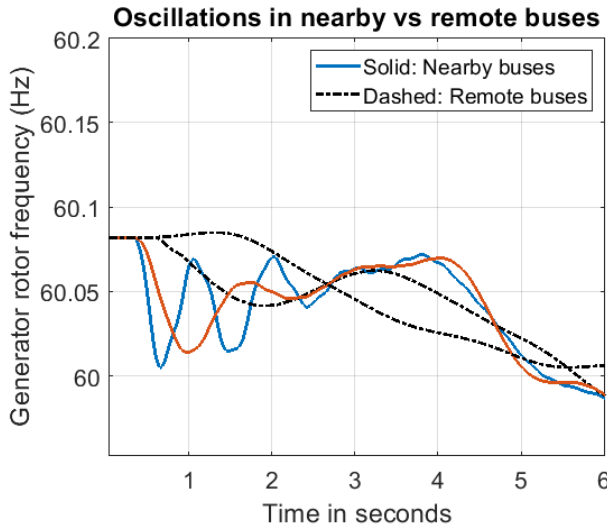


Fig. 1: Simulated loss of generation seen from nearby vs remote buses

for the nearby buses and relatively slow oscillations for the remote buses.

The presence of significant local modes for nearby events is verified from the ratio of the proposed J_{DFT} to $J_{\Delta f}$. Four loss of generation events estimated by FNET/GridEye server [6] are identified and the ratio of the maximum value of the indices versus the event location are plotted in Fig. 2.

- Estimated loss of 880 MW in St. Louis, MO on 02/07/2021
- Estimated loss of 630 MW in Brilliant, OH on 02/09/2021
- Estimated loss of 1400 MW in Louisville, KY on 02/16/2021
- Estimated loss of 1000 MW in Monroe, MI on 02/17/2021

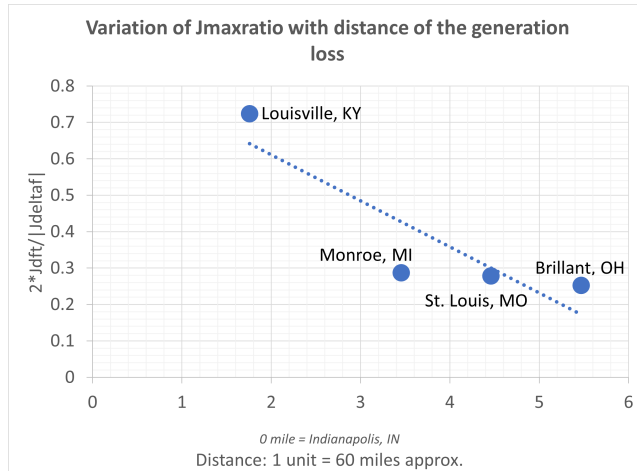


Fig. 2: Inverse correlation of the ratio of proposed indices with distance from generation losses

The effectiveness of the proposed indices to distinguish a nearby event is evident from the fact that their ratio tends to have an inverse correlation with the distance of the event location as seen in Fig. 2.

B. Illustration of indices during an event

The nearest event identified from the author's measurement location is the estimated 1400 MW loss of generation in Louisville, KY on Feb 16, 2021 which is plotted in Fig. 3. The index values are calculated every time stamp for the available measurements. Fig. 4 shows how the proposed $J_{\Delta f}$ measures the average change in frequency and the J_{DFT} measures the presence of 0.8 Hz oscillations. The indices reflect the loss of generation event around 8 seconds after it has occurred which is acceptable for the kind of UFLS scheme that we are proposing. For better visualization, Fig. 5 shows a time-aligned frequency and indices plots for 60 seconds of measurements.

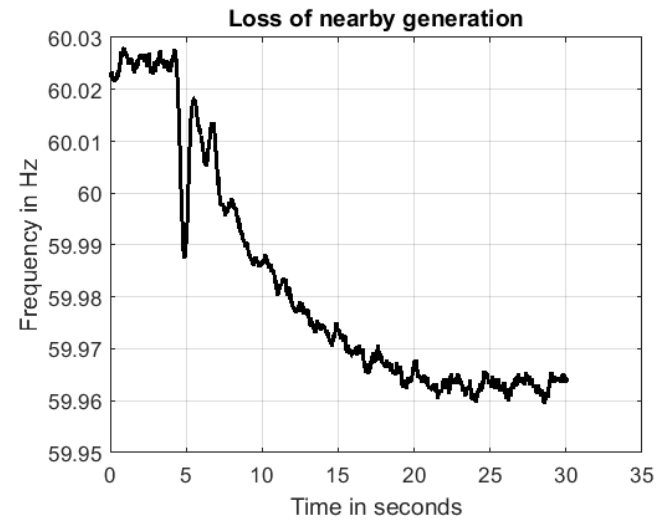


Fig. 3: Estimated 1400MW generator trip near Louisville

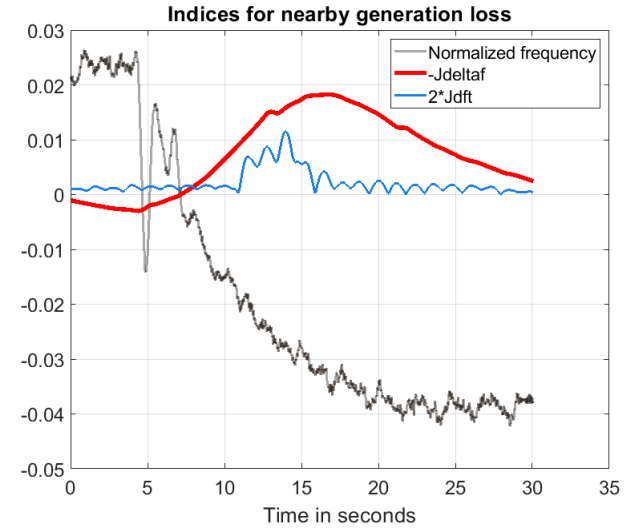


Fig. 4: Actual indices plot for the Louisville's trip

Fig. 6 shows normalized frequency and indices plot for an event with a marked decrease in frequency but lacking a pronounced oscillation around 0.8 Hz which probably corresponds to a loss of generation event far away from the measurement location.

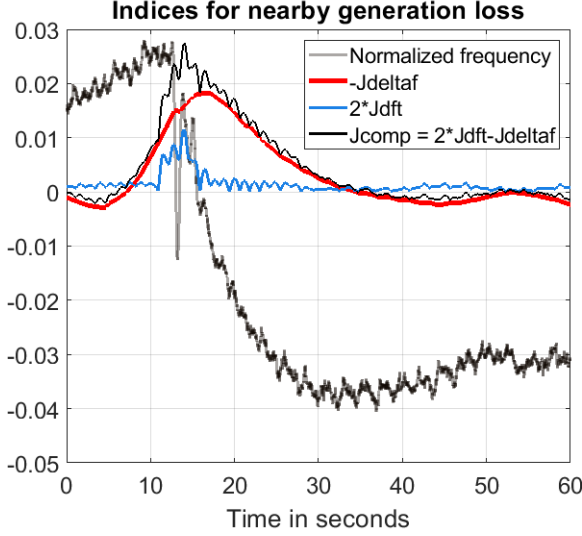


Fig. 5: Time-aligned indices plot for the Louisville's trip

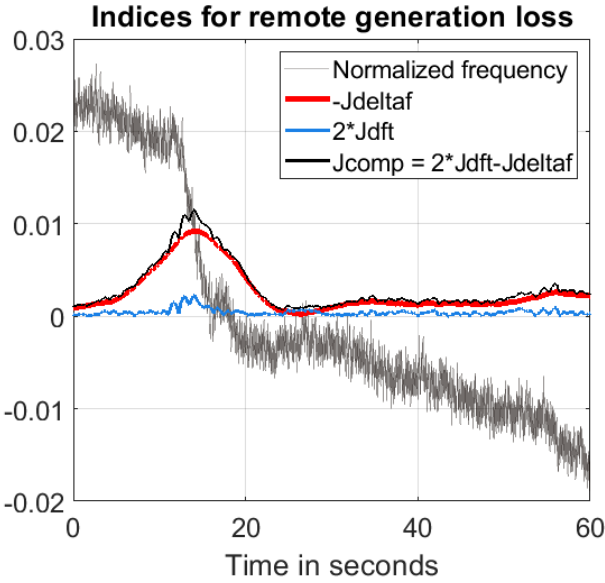


Fig. 6: Indices plot for remote generator trip

The DFT index-plot so far seems to precisely detect the 0.8 Hz oscillations but a much smoother curve is obtained using the J_{sinc} index. In Fig. 7, the J_{sinc} plot is scaled down to make it comparable with the J_{DFT} plot for the same event in Fig. 3.

C. Avoiding Detection of Frequency Impulses

The goal of this work is to detect loss of generation events rather than impulses or glitches such as shown in Fig. 8(a). This goal affects the choice of weights in a composite index such as $J_{comp} = \alpha J_{DFT} - \beta J_{\Delta f}$. When $\alpha = 2$ and $\beta = 1$ then the event shown in Fig. 8(a) has the highest value of J_{comp} during one particular 24 hour period. If the weight given to J_{DFT} is reduced to 0.5, the event shown in Fig. 8(b) has the highest composite index value in the same 24 hour period. As the work progresses, we are moving away

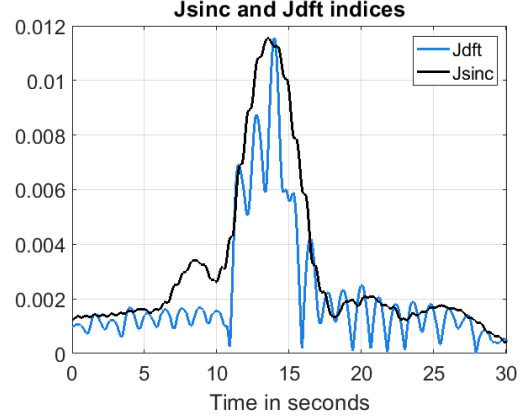


Fig. 7: J_{sinc} and J_{DFT} for the event in Fig.3

from applying a threshold to a single composite index such as J_{comp} in favor of applying multiple thresholds to multiple indices.

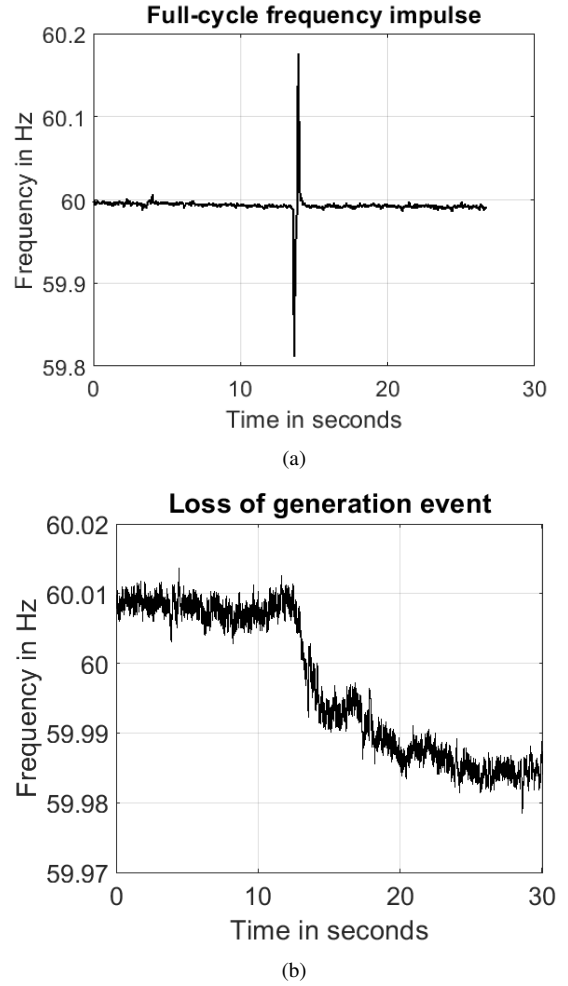


Fig. 8: Events detected using different values of weights in a composite index

IV. TRAINING DECISION TREES

Training decision trees requires a large amount of data in the form of input-output pairs. The authors have been collecting data from frequency measurements at Indianapolis during loss of generation events on the US eastern interconnection for years. Indices calculated from the measured data will be included in the input vector. More recently, the authors have acquired access to identifying information about grid events from FNET/GridEye to determine the output or target value of each input-output pair.

The input vector contains maximum values of indices calculated during a 120 second window of measurements containing an event reported by FNET/GridEye. The target assigned to each input vector in the training data is set to ‘1’ if the event is a nearby loss of generation and ‘0’ otherwise. For example, we set the target to ‘1’ if the event report from FNET/GridEye estimates an amount of generation loss greater than 400 MW and the location to be within about 100 miles of Indianapolis.

The resulting DTs will be used to shed load in response to nearby loss of generation events, and so far we only have one event in this category which is the estimated 1400 MW generation trip around Louisville. The composite index $J_{maxratio}$ plotted in Fig. 2 is defined as the ratio of time-aligned indices $(2J_{DFT})/|J_{\Delta f}|$ calculated at the time when the maximum value of J_{comp} occurs. The value of $J_{maxratio}$ for the event estimated by FNET/GridEye to have occurred near Louisville is greater than 0.7 while the value of $J_{maxratio}$ for other events is less than 0.3. The maximum value of $-J_{\Delta f}$ for this event is about 0.18 which means the maximum value of $-J_{\Delta f}$ for a 400 MW generation trip would be about $0.18 * 400/1400 = 0.05$. Based on this limited set of observations the criteria for detecting nearby loss of generation events greater than 400 MW could be $J_{maxratio} > 0.5$ and $J_{\Delta f} < -0.05$ as in Fig. 9. Eventually, the authors will accumulate a training set of event data where the input vector contains maximum values of several indices and use DT training software to determine the criteria for detecting nearby loss of generation events. Training decision trees for detecting loss of nearby generation is similar to previous work by authors using DTs for response based control in [12], [13].

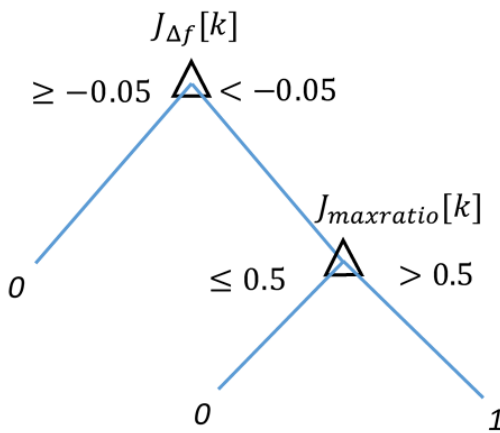


Fig. 9: An example DT to detect a nearby loss of generation

V. RECURSIVE ALGORITHM FOR MICRO-CONTROLLER IMPLEMENTATION

The indices in the previous section require large amounts of memory which makes them unsuitable for microcontroller implementation. In order to use microcontrollers for event detection we have derived recursive approximations to the indices [14].

A. Recursive approximation for $J_{\Delta f}$

A recursive form for $J_{\Delta f}$ index is obtained as follows.

$$J_{\Delta f}(t_{N+1}) = 0.9999 * J_{\Delta f}(t_N) + [f(t_{N+1}) - 2f(t_{N+1-Ns}) + f(t_{N+1-2Ns})]/Ns$$

The old index is multiplied by 0.9999 to ensure numerical stability. For the same event in Fig. 3, the recursive $J_{\Delta f}$ closely follows the non-recursive one as shown in Fig. 10.

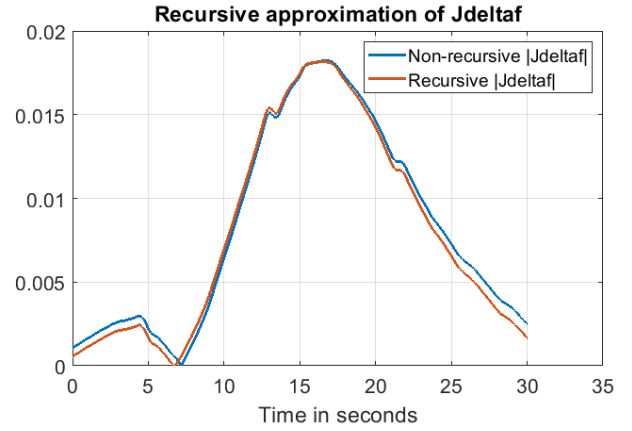


Fig. 10: Recursive approximation of $J_{\Delta f}$

B. Recursive approximation to J_{sinc}

The recursive form for J_{sinc} is approximated using a second order resonant transfer function. In order to approximate an ideal bandpass filter that passes frequencies in the range of $4 \text{ rad/s} < \omega < 6 \text{ rad/s}$, we choose pole locations close to $j\omega = 5j$ on the imaginary axis:

$$p_1 = -0.5 - 5j, \quad p_2 = -0.5 + 5j$$

The transfer function $\frac{25.25s}{s^2 + s + 25.25}$ is a band pass filter whose frequency response is plotted in Fig. 11. The magnitude is within 3 dB of its peak value between approximately 4.55 rad/s and 5.55 rad/s . The output of the transfer function is calculated by solving the following linear system using Euler's method:

$$\begin{bmatrix} x'_1 \\ x'_2 \end{bmatrix} = \begin{bmatrix} 0 & 1 \\ -25.25 & -1 \end{bmatrix} \begin{bmatrix} x_1 \\ x_2 \end{bmatrix} + \begin{bmatrix} 0 \\ 25.25 \end{bmatrix} f \quad (6)$$

The output of the bandpass filter is obtained from the second state variable, $V_{BP} = x_2$. The linear system in (6) has low damping and is designed to resonate in response to small deviations of frequency around 60 Hz. The resonant linear system experiences large, undesirable transients when there is

a large change in frequency which could occur during startup or any interruption of the frequency calculation. Therefore, it is necessary to limit the range of the values that are input to the linear system to a small range of interest:

$$f(t_N) = \begin{cases} 60.1 & ; f(t_N) > 60.1 \\ f(t_N) & ; 59.9 \leq f(t_N) \leq 60.1 \\ 59.9 & ; f(t_N) < 59.9 \end{cases} \quad (7)$$

The recursive *sinc* index $J_{sinc,rec}$ is then obtained as root mean square average of V_{BP} over 2.5 seconds.

$$J_{sinc,rec}(t_N) = \sqrt{\frac{\sum_{k=N-149}^N V_{BP}(t_k)^2}{150}} \quad (8)$$

The recursively calculated $J_{sinc,rec}$ for the event in Fig. 3 is shown in Fig. 12.

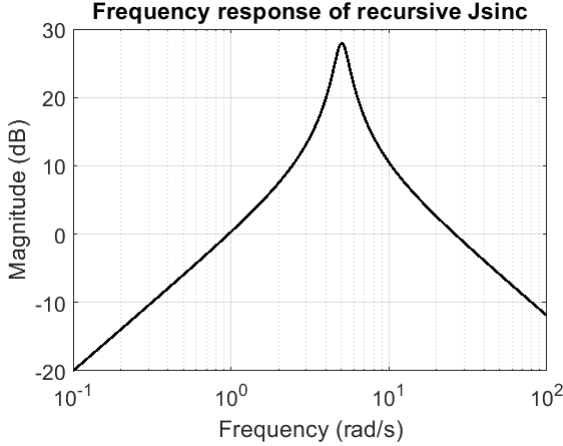


Fig. 11: Frequency response of $H(s) = \frac{25.25s}{s^2+s+25.25}$

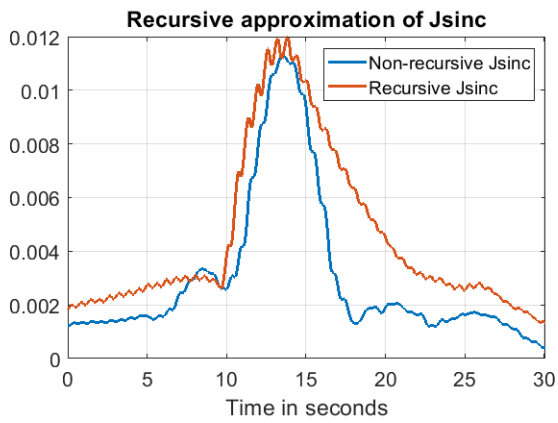


Fig. 12: Recursive approximation of J_{sinc}

VI. CONCLUSION

The paper proposes several indices to detect nearby loss of generation events useful for location targeted UFLS scheme. Pattern recognition tools like decision trees can continuously monitor these indices and decide whether a nearby loss of

generation event has just occurred. Such a supervised learning requires a large amount of data from known events or computer simulations.

The proposed UFLS strategy of detecting nearby loss of generation and disconnecting loads near loss of generation events is expected to minimize change in inter-area power flows and sometimes prevent relay's misoperation. The algorithms derived in this paper can be used by relatively non-critical standalone devices such as residential air conditioners and dryers to autonomously detect and temporarily shut themselves down for self-healing the grid. They do not require any communication with the utility. The length of the time for which the load is disconnected can be set around 10 minutes to allow independent system operators (ISOs) enough time to re-dispatch generation. Misoperation of the UFLS control is unlikely to cause harm to the power system because only a fraction of the loads would be controlled by the proposed relays. Noisy or missing phasor samples for real-time control can be handled using techniques described in the previous work in [15].

REFERENCES

- [1] M. Klein, G. J. Rogers, and P. Kundur, "A fundamental study of inter-area oscillations in power systems," *IEEE Transactions on Power Systems*, vol. 6, no. 3, pp. 914–921, 1991.
- [2] A. Allen, S. Santoso, and E. Muljadi, "Algorithm for screening phasor measurement unit data for power system events and categories and common characteristics for event seen in phasor measurement unit relative phase-angle differences and frequency signals," *NREL- Technical Report*, 2013.
- [3] S. Rovnyak, C. Taylor, J. Mechenbier, and J. Thorp, "Plans to demonstrate decision control tree using phasor measurements for hvdc fast power changes," *Faults and Disturbance Analysis and Precise Measurements in Power Systems Conference*, November 1995.
- [4] H. Bevrani, G. Ledwich, and J. J. Ford, "On the use of df/dt in power system emergency control," in *2009 IEEE/PES Power Systems Conference and Exposition*, 2009, pp. 1–6.
- [5] L. J. Shih, W. J. Lee, J. C. Gu, and Y. H. Moon, "Application of df/dt in power system protection and its implementation in microcontroller based intelligent load shedding relay," in *Conference Record. Industrial and Commercial Power Systems Technical Conference 1991*, 1991, pp. 11–17.
- [6] Y. Zhang, P. Markham, T. Xia, L. Chen, Y. Ye, Z. Wu, Z. Yuan, L. Wang, J. Bank, J. Burgett, R. W. Connors, and Y. Liu, "Wide-area frequency monitoring network (fnet) architecture and applications," *IEEE Transactions on Smart Grid*, vol. 1, no. 2, pp. 159–167, 2010.
- [7] Yong Sheng and S. M. Rovnyak, "Decision trees and wavelet analysis for power transformer protection," *IEEE Transactions on Power Delivery*, vol. 17, no. 2, pp. 429–433, 2002.
- [8] Zhi Shi, Li-Yuan Deng, and Qing-Jiang Chen, "Numerical solution of differential equations by using haar wavelets," in *2007 International Conference on Wavelet Analysis and Pattern Recognition*, vol. 3, 2007, pp. 1039–1044.
- [9] S. M. Rovnyak, S. Koskie, Yong Sheng, V. S. Rajput, and Xiaohui Hu, "Laboratory testing of a distributed generator unintentional islanding detection scheme," in *2008 IEEE Power and Energy Society General Meeting - Conversion and Delivery of Electrical Energy in the 21st Century*, 2008, pp. 1–6.
- [10] A. Bykhovsky and J. Chow, "Power system disturbance identification from recorded dynamic data at the northfield substation," *International Journal of Electrical Power and Energy Systems*, vol. 25, pp. 787–795, 2003.
- [11] K. Mei, S. M. Rovnyak, and C. Ong, "Clustering-based dynamic event location using wide-area phasor measurements," *IEEE Transactions on Power Systems*, vol. 23, no. 2, pp. 673–679, 2008.
- [12] Q. Gao and S. M. Rovnyak, "Decision trees using synchronized phasor measurements for wide-area response based control," *IEEE Transactions on Power System*, vol. 26, May 2011.

- [13] S. M. Rovnyak, D. W. Longbottom, D. C. Vasquez, and M. N. Nilchi, *Chapter 8: Response-Based Event Detection for One Shot Wide-Area Stability Controls.* Monitoring and Control using Synchrophasors in Power Systems with Renewables, *edited by Innocent Kamwa and Chao Lu.*, The Institution of Engineering and Technology, ch. 978-1-78561-477-4 (print)/978-1-78561-478-1(ebook).
- [14] V. S. Rajput, S. M. Rovnyak, S. Koskie, and Yong Sheng, “A microcontroller-based phasor measurement system with can bus communication,” in *2008 IEEE Power and Energy Society General Meeting - Conversion and Delivery of Electrical Energy in the 21st Century*, 2008, pp. 1–5.
- [15] N. Dahal and S. Rovnyak, “Performance of response-based one shot control handling missing phasor measurements,” *IEEE PES General Meeting 2020*, September 2020.